LBL-35574
UC-410

Lawrence Berkeley Laboratory
UNIVERSITY OF CALIFORNIA

Accelerator & Fusion
Research Division

Presented at the SRI Conference, Upton, NY, July 18–22, 1994,
and to be published in the Proceedings

A Beamline for Macromolecular Crystallography at the Advanced Light Source

H.A. Padmore, T. Earnest, S.-H. Kim, A.C. Thompson,
and A.L. Robinson

August 1994

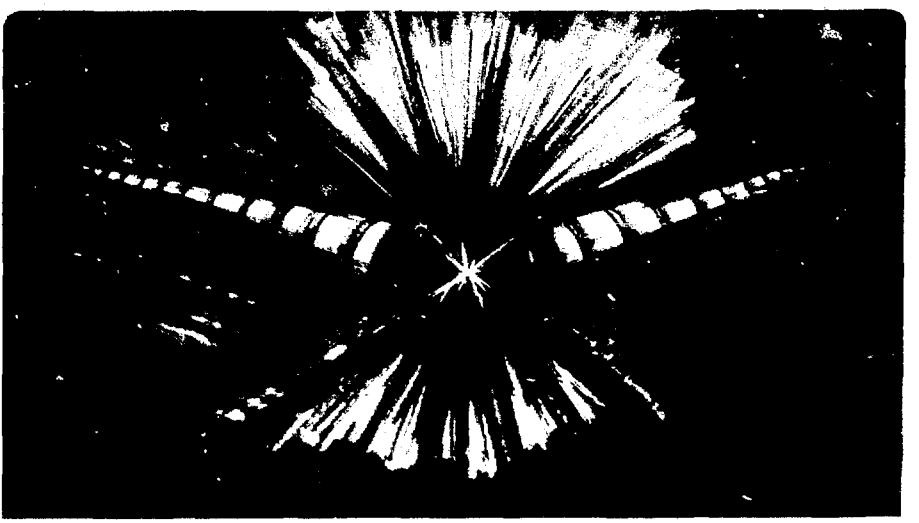

Prepared for the U.S. Department of Energy under Contract Number DE-AC03-76SF00098

LBL-35574
UC-410

A BEAMLINE FOR MACROMOLECULAR CRYSTALLOGRAPHY AT THE ADVANCED LIGHT SOURCE

H. A. Padmore, T. Earnest, S.-H. Kim, A. C. Thompson, and A. L. Robinson

Lawrence Berkeley Laboratory
University of California
Berkeley, CA 94720

AUGUST 1994

ACKNOWLEDGMENT - ***Work supported by the Director, Office of Energy Research, Office of Basic Energy Sciences, Materials Sciences Division of the U.S. Department of Energy, under Contract No. DE-AC03-76SF00098.**

A Beamline for Macromolecular Crystallography at the Advanced Light Source

H. A. Padmore, T. Earnest, S. - H. Kim, A. C. Thompson, and A. L. Robinson

Lawrence Berkeley Laboratory, University of California, Berkeley, CA 94720, USA

Abstract

A beamline for macromolecular crystallography has been designed for the ALS. The source will be a 37-pole wiggler with a 2-T on-axis peak field. The wiggler will illuminate three beamlines, each accepting 3 mrad of horizontal aperture. The central beamline will primarily be used for multiple-wavelength anomalous dispersion measurements in the wavelength range from 4 to 0.9 Å. The beamline optics will comprise a double-crystal monochromator with a collimating pre-mirror and a double-focusing mirror after the monochromator. The two side stations will be used for fixed-wavelength experiments within the wavelength range from 1.5 to 0.95 Å. The optics will consist of a conventional vertically focusing cylindrical mirror followed by an asymmetrically cut curved-crystal monochromator. This paper presents details of the optimization of the wiggler source for crystallography, gives a description of the beamline configuration, and discusses the reasons for the choices made.

Introduction

Measurements in macromolecular crystallography demand a high photon flux incident on the sample because of the weak diffraction often found from many crystals and because of the time needed to record many rotations of the crystal. The samples themselves are usually small, typically a few hundred microns. The required angular resolution of the x-ray beam at the crystal is set by the need to resolve adjacent diffraction orders and is dependent on the wavelength, the unit cell size, and the natural mosaicity of the sample. The product of the sample size and the required angular resolution sets the sample phase-space acceptance. A typical acceptance is 1 mm·mrad, for exampale for a crystal size of 1/3 mm and an angular resolution of 3 mrad. Consideration of the sample requirements in this way allows us to design the source and optics to optimize the flux integrated within the acceptance phase space,

rather than optimizing parameters, such as angular flux density and central brightness, that are not directly related to the flux impinging on the sample within the allowed angular resolution.

In this paper, we describe the methods that have been used to optimize the wiggler source, based on integrating over a defined phase space area. Once the source has been optimized, the details of the source position and angle characteristics can be examined in detail by integration over the relevant parts of the two-dimensional phase-space distribution. This analysis yields, for example, the position distribution integrated over a selected angular range. This result is important to understand because a multipole wiggler is a long incoherent source, and the effects of the depth of field are manifested by highly non-gaussian phase-space distributions.

With a detailed understanding of the optical properties of the source, the optical arrangement can be designed in an optimum way. Another influence on the optical design is the type and operation of the detector. In a previous design study, we considered using three beamlines in a multiplexed manner (i.e., the three beamlines would share the same central aperture but would time-share access to the beam). The beamlines were based on two curved-crystal monochromators focusing light from the central axis at a high angle, followed on the same central axis by a double-crystal monochromator. The multiplexing was to have been accomplished by vertically inserting and retracting the two curved-crystal monochromators. The reason for this choice of operation was based on the readout time of the proposed image-plate detector system, which had a typical readout time of 5 minutes. It is expected that typical crystals will require less than 10 seconds of exposure per rotation, so that, with an image-plate system, there was clearly a mismatch between the readout and exposure times. A multiplexing system would increase the overall data collection efficiency of the three beamlines. However, CCD detector systems have now been developed to the point where they have significant performance advantages over image plates. Readout times for the latest CCD cameras are typically only a few seconds, and these cameras have excellent dynamic range and sensitivity [1-3]. Since this readout time is less than the typical single rotation exposure time, multiplexing is no longer a worthwhile option. Because we will now use state-of-the-art CCD detectors systems [4], we have examined the possibility of using three beamlines operating in a simultaneous mode. The implications of doing this are examined in a later section of this paper and an optimum arrangement for the beamlines is described.

Optimization of the wiggler source

The first stage in the optimization of the wiggler source is to calculate its horizontal phase-space distribution. For wigglers in third-generation storage rings, the vertical phase-space area is much smaller than the sample phase-space acceptance and only the horizontal plane needs to be considered. The source-depth broadening of the vertical source size is relatively small, owing to the very small opening angle in the vertical plane at high photon energies.

The horizontal phase-space distribution is calculated by tracking the trajectory of an electron through the magnetic structure of the wiggler. Each point on the trajectory is characterized by local parameters: vertical field strength, position perpendicular to the central axis of the device, and tangential angle of the trajectory. With a knowledge of the local magnetic field and the machine electron energy, the flux radiated between adjacent points on the trajectory can be calculated. Because an optical system will usually focus to a fixed position of a device such as a slit, the position of the slit can be considered as being transformed back to the source. Clearly, to maximize the flux through the slit, the optical system will be designed to transform the slit position back to the longitudinal center of the source. The local emission coordinates of an electron can be transformed to this plane, and the flux radiated between adjacent points can be allocated to a particular position and angle space. At each point on the trajectory, a convolution over the position and angle distribution of the electron beam source is performed. The result for tracking over the whole length of the wiggler is the phase-space distribution [5-7]. Fig. 1 shows such a distribution at an observation wavelength of 1 Å for a 37-pole, 2-T wiggler with the ALS operating at 1.5 GeV. It can be seen that the distribution is highly non-gaussian and that observation at angles off the optical axis will lead to a large apparent source size. The example shown here assumes a sinusoidal field, but in reality the fieldincludes higher harmonics that distort the trajectory. Therefore, we have calculated the actual field and trajectory to predict the effects of this distortion for a range of cases.

Having obtained the phase-space distribution, the flux integrated through a defined phase space can be calculated. Although the phase-space area is defined, the aspect ratio defining the optical magnification of an imaging system is a free parameter that must be selected to maximize the flux integral. Having calculated the flux integral, the system can be optimized by altering the magnetic structure. For the protein-crystallography wiggler, the maximum length is defined by mechanical constraints to be 3 m; the minimum magnetic gap is defined

by consideration of the dependence of the electron beam lifetime on vertical aperture to be 14 mm; but there is a free choice of the number of poles. Either a large number of weak-field poles or a smaller number of strong-field poles can be used. The model used to determine the relationship between the on-axis field and the gap-to-period ratio is that for a hybrid structure with vanadium permendur pole pieces and NdFeB magnets [8]. The result of changing the number of poles in our fixed-length wiggler, with a machine electron energy of 1.5 GeV and an observation wavelength of 1 Å, is shown in Fig. 2 for a range of phase-space areas. It can be seen that the peak flux occurs at 37 poles for typical phase-space acceptances near 1 mm·mrad. A full description of the wiggler can be found in [9].

The resulting phase-space distribution can now be used to examine the detailed optical properties of the source. An example is shown in Fig. 3, where the position distribution is shown for horizontal collection apertures of 3 mrad both for the on-axis position and for a position 3 mrad off-axis. In this case, a horizontal emittance of 10^{-8} m·rad was used, giving an electron beam size of 0.77 mm (FWHM). The apparent FWHM optical beam size, even for the on-axis case, has increased to 1.7 mm and, for the off-axis case, is severely broadened to 7.5 mm. This broadening is due to the depth of the source and the finite collection aperture. Viewing on-axis and collecting a vanishingly small aperture, we would see the actual electron beam size.

The phase-space method can also be used to examine the flux integrated in a certain phase space area for sources at different synchrotron facilities. This comparison has been done for several sources in order to extrapolate from known data-collection times for otherbeamlines to the case of the ALS, as well as to demonstrate that the ALS system will be fully competitive. The results are shown in Table 1. Extrapolating from the existing beamlines listed, we can be confident that our average data-collection time per typical rotation will be less than 10 seconds. Going much faster than this will lead to diminishing returns, owing to the finite readout time of our CCD detectors.

Beamline configuration

The optical characteristics of the central and side fans of radiation are clearly very different and different optical solutions have to be adopted in each case. Fig. 4 shows the layout for the

the optical arrangement we have adopted. Three beamlines will be constructed, each taking 3 mrad of horizontal aperture. The central station will be a conventional double-crystal arrangement with a vertically collimating pre-mirror and a double-focusing mirror after the monochromator. The first crystal will have a pin-post cooling arrangement. This beamline will be used for multiple-wavelength anomalous dispersion, and the main requirements for the monochromator are for high resolution with rapid and repeatable wavelength changing. The focused light spot sizes at the sample collimator will be 1.0 and 0.4 mm in the horizontal and vertical directions, respectively.

The side stations will have a vertically focusing mirror followed by a curved-crystal monochromator. This arrangement is based on the commonly used geometry introduced by Lemonnier et al. [10] and developed by many groups [for example, see references 11 and 12 and references in 13]. The curved-crystal monochromators will be identical and will have an asymmetric-cut arrangement with a nominal compression factor of 10. As the wavelength is changed, however, the required crystal radius will change, as will the image position, to stay at the Guinier position. To obtain a reasonably small change of image distance over the design wavelength of 1.5 to 0.95 Å, three crystals will be used with asymmetry angles from 7.5 to 10.6 degrees for Si(111). With a source distance of 14.1 m, the image distance will vary from 1.04 to 2.0 m around its nominal value of 1.4 m. The pre-mirrors will be located inside the shield wall at 10.6 m from the source and will give a variable demagnification from 2.2:1 to 1.7:1 to cover this focal plane movement. The extended horizontal source will be demagnified to around 0.75 mm at the center of the wavelength range for each asymmetric cut. In the vertical direction, the electron beam size at a nominal vertical emittance of 10^{-9} m·rad will be 0.15 mm (FWHM), but will be increased by the source-depth effect at 1 Å wavelength to 0.25 mm (FWHM). At the nominal demagnification of 2.1:1, the spherical aberration of the mirror will increase the geometrical image size slightly to 0.15 mm (FWHM).

The M1 and M2 mirrors will be housed in a common vacuum tank, as will the curved-crystal monochromators C1 and C2. As beam for the central station passes between the two side stations, it is important that the M1 and M2 mirrors be usable almost up to their edges in the lateral direction and that the mirror bending be actuated from the ends and back so that no part of the central beam is obscured. For the same reason, the beam from the two curved crystals crosses over so that the bending mechanisms are on the outside of the beam fan. As stated in the previous section, the apparent beam size in the on-axis position (collecting 3

mrad) is 1.7 mm ((FWHM), considerably smaller than in the sidestation positions, so provision has been made to translate either of the side stations into the central-station position for experiments that require the highest brightness. This movement will obscure the central station position. In this case, taking into account optical aberrations, the demagnification and the angular dispersion of the diffracted beam [10], the horizontal image size will be 0.3 mm (FWHM).

Project Status.

Construction of the wiggler has started and is expected to be completed in October 1995. The mechanical design of key parts of the beamline, such as the high-power curved-crystal monochromator, has also started, and prototypes will be produced over the next six-month period. The power radiated by the wiggler into each 3-mrad aperture will be around 2.6 KW. From examination of other high power beamlines with similar characteristics (for example X25 at NSLS, [14, 15]), we have been able to determine that there are many techniques that have been successfully applied to optical systems to preserve the source brightness. We are confident that similar methods, together with thorough finite-element thermal calculations, will allow us to overcome the high heat-load problems on this beamline. Funding of the beamline (total capital cost $8.8 million) is expected in October 1994; first beam into one of the side station lines will be in May 1996; and completion of the project will be in May 1997. The construction of a support laboratory for structural biology has been funded ($7.9 million); the laboratory will be completed by September 1995 and fully equipped by September 1996.

Acknowledgment

This work has benefited from advice from many people, but in particular we wish to acknowledge helpful discussions with Colin Nave, Wayne Hendrickson, Craig Ogata, Steve Ginnell, Lisa Keefe, Randy Alkire, Bob Sweet, Lonny Berman, Don Bilderback, Joe Navaie, Steve Ealick, Ed Westbrook, Gerd Rosenbaum, Keith Hodgson, Paul Phizackerly, Jon Cerino, Tom Rabedeau and Andy Sabersky.

This work was supported by the Director, Office of Energy Research, Office of Basic Energy Sciences, Materials Sciences Division of the U.S. Department of Energy, under Contract no. DE-AC03-76SF00098.

References

1. M. G. Strauss, E. M. Westbrook, I. Naday, T. A. Coleman, M. L. Westbrook, D. J. Travis, R. M. Sweet, J. W. Pflugrath, M. Stanton, Nucl. Instrum. Meth. A297 (1990) 275.

2. M. Stanton, Nucl. Instrum. Meth. A325 (1993) 550.

3. M. Stanton, W. C. Phillips, D. O'Mara, I. Naday, and E. M. Westbrook, Nucl. Instrum. Meth. A325 (1993) 558.

4. We will use the 'Gold Detector' to be built by the group of Ed Westbrook, Structural Biology Center, Argonne National Laboratory.

5. R. Coisson, S. Guiducci and M. A. Preger, Nucl. Instrum. Meth. 201 (1982) 3.

6. R. Coisson and R. P. Walker, Proc. SPIE, 582 (1985) 24.

7. G. E. van Dorssen, H. A. Padmore, and W. Joho, SPIE, 2013, (1993).

8. K. Halbach, Nucl. Instrum. Meth. 187 (1981) 109.

9. E. Hoyer, J. Akre, D. Humphries, S. Marks, Y. Minamihara, P. Pipersky, D. Plate, and R. Schlueter, these proceedings.

10. M. Lemonnier, R. Fourme, F. Rousseaux, and R. Kahn, Nucl. Instrum. Meth. 152 (1978) 173.

11. J. R. Helliwell, T. J. Greenhough, P. D. Carr, S. A. Rule, P. R. Moore, A. W. Thompson, and J. S. Worgan, J. Phys. E. 15 (1982) 1363.

12. J. R. Helliwell, M. Z. Papiz, I. D. Glover, J. Habash, A. W. Thompson, P. R. Moore, N. Harris, D. Croft, and E. Pantos, Nucl. Instrum. Meth. 246 (1986) 617.

13. Macromolecular Crystallography with Synchrotron Radiation', Cambridge Univ. Press, 1992, J. R. Helliwell

14. L. E. Berman, J. B. Hastings, T. Oversluizen, and M. Woodle, Rev. Sci. Instrum. 63(1) (1992) 428.

15. L. E. Berman and J. B. Hastings, SPIE, 1739 (1992) 489.

Figure Captions

Fig. 1

Horizontal phase-space diagram for a 37-pole wiggler with a peak on-axis field of 2T and a period 16 cm. The electron beam energy is 1.5 GeV and the observation wavelength is 1 Å. The horizontal electron beam size is 0.77 mm (FWHM)

Fig. 2

The variation in wiggler flux at 1Å integrated into phase-space areas from 0.25 to 8.0 mm·mrad as a function of the number of poles in a fixed length of 3 m. The assumed magnetic gap is 14 mm.

Fig. 3

The apparent horizontal source size for collection apertures of 3 mrad for the on-axis position (a) and for a position with a center line 3 mrad off axis (b).

Fig. 4

Optical configuration of the beamline showing two identical curved-crystal monochromator side stations and a central double-crystal monochromator for multiple-wavelength anomalous dispersion measurements.

Table 1.

Comparison of representative sources for macromolecular crystallography. Note that a phase space area of 1 mm·mrad is used and that the observation wavelength is 1 Å.

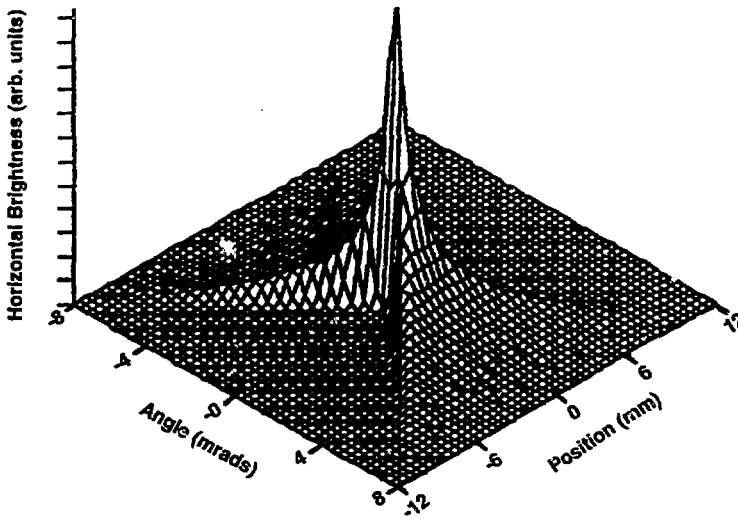
Horizontal Brightness (arb. units)
-8
-4
0
4
8
Angle (mrads)
-12
-6
0
6
12
Position (mm)

Figure 1

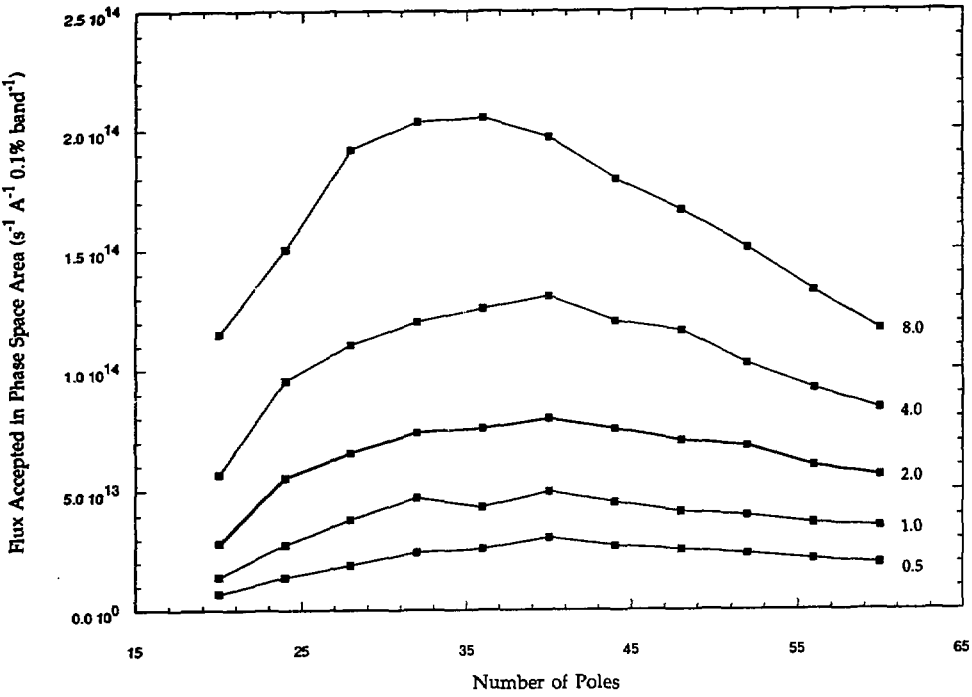
Flux Accepted in Phase Space Area (s^{-1} A^{-1} 0.1% $band^{-1}$)
2.5 10^{14}
2.0 10^{14}
1.5 10^{14}
1.0 10^{14}
5.0 10^{13}
0.0 10^{0}
15
25
35
45
55
65
Number of Poles
8.0
4.0
2.0
1.0
0.5

Figure 2

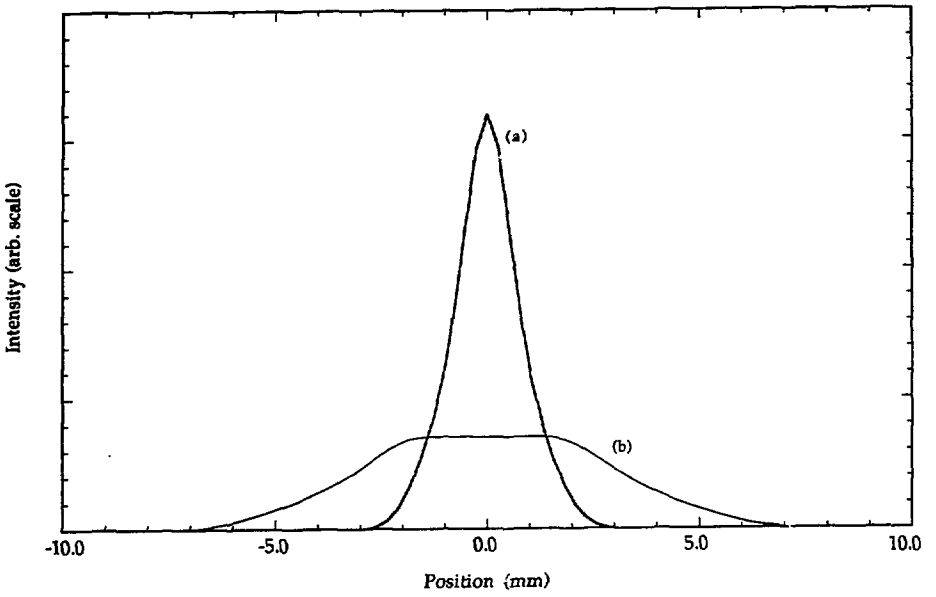

Figure 3

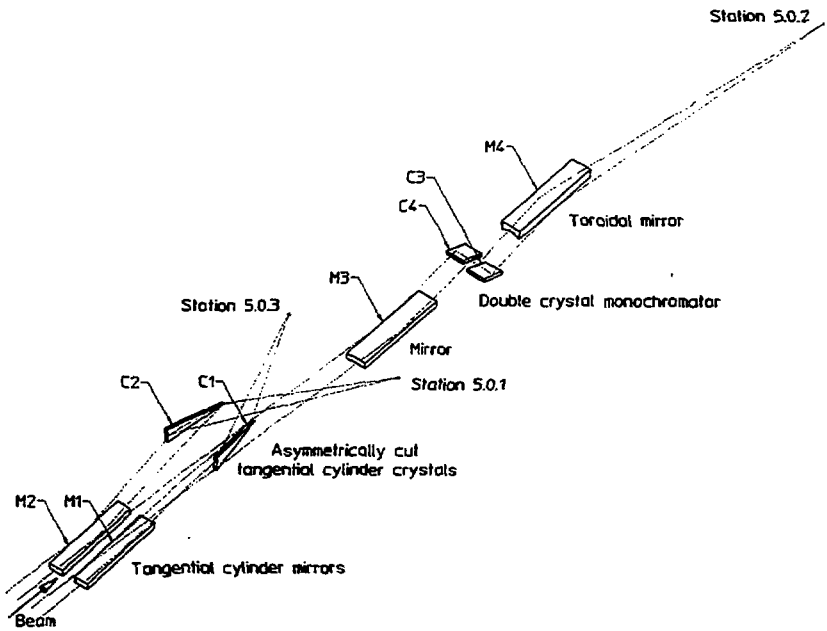
Station 5.0.2
M4
C3
C4
Toroidal mirror
M3
Station 5.0.3
Double crystal monochromator
Mirror
C2
C1
Station 5.0.1
Asymmetrically cut
tangential cylinder crystals
M2
M1
Tangential cylinder mirrors
Beam

Figure 4

Facility	ALS	ALS	NSLS	SRS	APS
Energy (GeV)	1.9	1.5	2.5	2.0	7.0
Beamline	5.0.2	5.0.2	X13C	9.5	bend magnet
Field (T)	2.0	2.0	1.2	5.0	0.6
Period (cm)	16.0	16.0	bend magnet	wavelength shifter	bend magnet
No. poles	37	37	1	1	1
Current (A)	0.4	0.4	0.25	0.25	0.1
Flux @ 1Å in 1 mm-mrad (photons/s)	8×10^{13}	1.5×10^{13}	0.27×10^{13}	0.45×10^{13}	6×10^{13}

Facility	APS	APS	NSLS	SSRL	SSRL	CHESS
Energy (GeV)	7.0	7.0	2.5	3.0	3.0	5.4
Beamline	wiggler A	undulator A	X25	7.1	9.2	F1
Field (T)	1.0	K=2.2, n=3	1.1	1.8	1.9	1.2
Period (cm)	15.0	3.3	12.0	45.0	25.0	19.6
No. poles	20	152	27	8	16	25
Current (A)	0.1	0.1	0.25	0.1	0.1	0.1
Flux @ 1Å in 1 mm-mrad (photons/s)	30×10^{13}	50×10^{13}	5.0×10^{13}	0.72×10^{13}	1.6×10^{13}	8.8×10^{13}

Table 1